Distinct structure and activity recoveries reveal differences in metal binding between mammalian and *Escherichia coli* alkaline phosphatases

Le ZHANG[1], René BUCHET and Gérard AZZAR†

UFR de Chimie-Biochimie, CNRS-UMR 5013, Université Claude Bernard Lyon 1, 43 Boulevard du 11 Novembre 1918, 69622 Villeurbanne Cedex, France

The amino acids involved in the coordination of two Zn^{2+} ions and one Mg^{2+} ion in the active site are well conserved from EAP (*Escherichia coli* alkaline phosphatase) to BIAP (bovine intestinal alkaline phosphatase), whereas most of their surrounding residues are different. To verify the consequences of this heterology on their specific activities, we compared the activity and structure recoveries of the metal-free forms (apo) of EAP and of BIAP. In the present study, we found that although the sensitivities of EAP and BIAP to ions remained similar, significant differences in dimeric structure stability of apo-enzymes were observed between EAP and BIAP, as well as in the kinetics of their activity and secondary structure recoveries. After mild chelation inactive apo-EAP was monomeric under mild denaturing conditions, whereas inactive apo-BIAP remained dimeric, indicating that the monomer–monomer contact was stronger in the mammalian enzyme. Dimeric apo-EAP (0.45 μM, corresponding to 4 units/ml) recovered approx. 80 % of its initial activity after 3 min incubation in an optimal recovery medium containing 5 μM Zn^{2+} and 5 mM Mg^{2+}, whereas dimeric apo-BIAP (0.016 μM, corresponding to 4 units/ml) recovered 80 % of its native activity after 6 h incubation in an optimal recovery medium containing 0.5 μM Zn^{2+} and 5 mM Mg^{2+}. Small and different secondary structure changes were also observed during activity recoveries of apo-BIAP and apo-EAP, which were not in parallel with the activity recoveries, suggesting that distinct and subtle structural changes are required for their optimal activity recoveries.

Key words: alkaline phosphatase, apo-enzyme, ion-binding, activity recovery, structure recovery.

INTRODUCTION

Alkaline phosphatases (E.C.3.1.3.1) belong to a family of homodimeric metalloenzymes common to all living organisms [1]. Alkaline phosphatase catalyses the hydrolysis of phosphomonoesters at alkaline pH, by forming inorganic phosphate and alcohol [2]. This enzymatic activity is ensured by the participation of Zn^{2+} and Mg^{2+} ions. In EAP (*Escherichia coli* alkaline phosphatase), each active site contains three cation-binding sites (M1, M2 and M3) (Figure 1) [3,4]. The numbering of the active site follows the increasing affinities of the sites for their ions [5]. The M1 site binds Zn^{2+} very strongly, due to the coordination of Zn^{2+} with two histidine residues, whereas the M2 site has only one histidine residue and a slight preference for Zn^{2+} over Mg^{2+} [6]. At a high Mg^{2+} concentration, the Mg^{2+} ion may displace the Zn^{2+} ion from the M2 site, without greatly affecting its overall activity (k_{cat}/K_m) [5,6]. Although the M3 site is the less specific among these three binding sites, an Mg^{2+} ion in this site is essential for the stability and the activity of EAP [7–10].

There is only one EAP, but four alkaline phosphatase isoenzymes, that have been isolated in humans. Three of them are tissue-specific (placenta, intestinal and germinal) [11–13] and one which is tissue non-specific can be found in liver, kidney and bone [14]. Moreover, at least seven isoenzymes of intestinal alkaline phosphatase have been revealed in BIAP (bovine intestinal alkaline phosphatase) [15]. Mammalian alkaline phosphatases are membrane-bound proteins containing a glycosylphosphatidyl inositol anchor [16]. The amino acids involved in the coordination of two Zn^{2+} ions and one Mg^{2+} ion with the catalytic serine in the active site are well conserved from EAP [3,4] to human placental alkaline phosphatase [17], whereas most of the surrounding residues are different. Only 25–30 % similarity was observed between the amino acid sequence of EAP [18] and that of mammalian alkaline phosphatases, although a 90–98 % similarity has been found between the four isoforms of human alkaline phosphatase [19,20].

Except for the distinct amino acid sequences between the prokaryotic EAP and the eukaryotic alkaline phosphatases, other differences in structure and activity levels have been reported. EAP is thermostable over a large temperature range ($T_m = 95$ °C) ([9,21]), but has a relatively low enzymatic activity. The mammalian enzymes have 10 to 100 times higher specific activities than EAP [20]. However, they are much more sensitive to thermal denaturation ($T_m = 65$ °C) [20,22]. Mammalian alkaline phosphatases possess additional secondary structure elements that are not present in EAP, including an interfacial-crown-domain which is formed by the insertion of an approx. 60 residue segment from each monomer, a calcium-binding domain and an N-terminal α-helix in each monomer, which forms an arm embracing the other monomer [17,20,23]. These elements have been shown to play important roles in defining the overall stability and in modulating the catalytic parameters of mammalian alkaline phosphatases [17,20,23–25]. The cooperativity found between subunits in EAP and mammalian alkaline phosphatases is different during enzymatic activity. Both positive and negative cooperativities, related to ion-binding and to phosphate-binding respectively, were observed in the case of EAP [21,26,27]. However, the placental mammalian alkaline phosphatases are non-cooperative allosteric enzymes and the two monomers of dimeric protein act independently during catalysis [28].

Abbreviations used: BCIP, bromochloro-indolyl phosphate; BIAP, bovine intestinal alkaline phosphatase; COBSI, change of backbone structure and interaction index; EAP, *Escherichia Coli* alkaline phosphatase; ICP-AES, inductively coupled plasma atomic emission spectroscopy; NBT, nitroblue tetrazolium; PNPP, *p*-nitrophenyl phosphate.

[1] To whom correspondence should be addressed (email le-zhang@hotmail.com).

† Deceased.

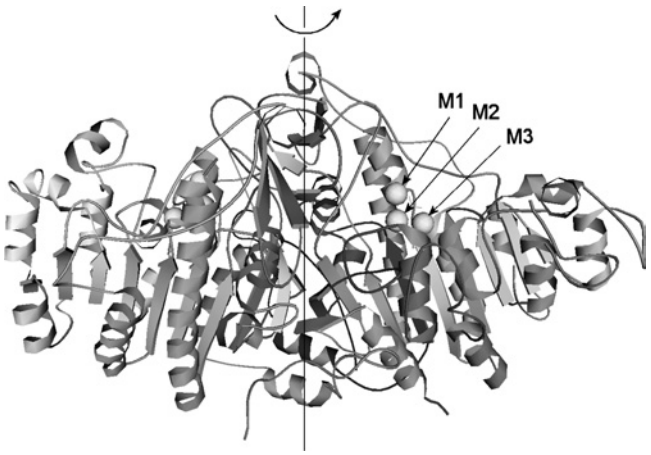

Figure 1 Ribbon diagram of EAP structure with three metal-binding sites (M1, M2 and M3) indicated in one monomer active-site

This Figure was produced from the structure data of the alkaline phophatase of *E. coli* in the Protein Data Bank (1ALK) using the VRML (virtual reality modeling language) program [4].

Previous findings indicated that the origin of the difference in specific activity between mammalian and prokaryotic enzymes may lie in differences in the environment of the active site, since the amino acid residues which do not participate directly in ion-binding are poorly conserved. To further investigate the differences in the active sites, we compared the activity and structure recovery of the metal-free forms of BIAP and prokaryote EAP. Significant differences in secondary structure recoveries of apo-enzymes were observed between the mammalian and prokaryotic enzymes, as well as in their activity recoveries.

EXPERIMENTAL

Materials

Alkaline phosphatase from bovine intestinal mucosa (BIAP, type VII-S) and EAP were purchased from Sigma (St. Louis, U.S.A.) and used without further purification. Enzymes were judged to be at least 98 % pure by molecular sieve chromatography, SDS/PAGE or MS (Mass Spectrometry Laboratory, Institute of Biochemistry and Biophysics, Warszawa, Poland). The result of MS indicated that the commercial BIAP contained mainly BIAP type III, at a sequence coverage of approx. 50 %. This analysis also indicated the presence of trace amounts of BIAP type IV, however, it was only matched based on similarity to BIAP type III and there was no peptide sequence specific to BIAP type IV. The specific activity of EAP was close to 100 units/mg of protein, whereas the specific activity of BIAP was close to 2000 units/mg of protein, as determined by alkaline phosphatase activity assay (as described below).

Alkaline phosphatase activity assay

Alkaline phosphatase activities were determined using the standard spectrophotometric assay. A 5 μl aliquot was added to 2 ml of the reactive solution containing 25 mM glycine and 10 mM PNPP (*p*-nitrophenyl phosphate), pH 10.4. The change in absorbance, due to the release of *p*-nitrophenolate at 37 °C, was monitored at 420 nm ($\varepsilon = 18.5\ cm^{-1} \cdot mM^{-1}$). One unit of alkaline phosphatase activity was defined as the amount of enzyme hydrolysing 1 μmol of PNPP per min under the described conditions.

Preparation of metal-free buffers

All buffers and enzyme solutions were prepared using metal-free water purchased from Merck KGaA (Darmstadt, Germany). All glassware and plastic tubes were prepared by washing in 1 % HCl, followed by a thorough rinsing in metal-free water.

Preparation of apo-enzyme stock solution

EAP and BIAP used in these experiments were first rendered metal-free (apo) by incubation of the enzyme (0.5 mg/ml) with 2 mM EDTA in metal-free 20 mM Tris buffer, pH 7.4 (mild chelation). The final activity of apo-enzyme was less than 0.5 % of holoalkaline phosphatase. Filtration using a Centricon-30 and washing were repeated several times to ensure that the final EDTA concentration was sub-nanomolar and that the amount of Tris-citrate and other salts from the commercial preparation was negligible. The apo-enzyme stock solution was concentrated to 20 mg/ml (corresponding to a 0.3 mM BIAP monomer with 64 kDa apparent molecular mass or a 0.4 mM EAP monomer with 45 kDa apparent molecular mass) and stored at 4 °C. Protein concentrations were determined by the method of Bradford [29]. Before use apo-enzymes were diluted in metal-free Tris buffer at a concentration corresponding to 4 or 15 units/ml activity of holoenzyme as indicated in the Figures.

Ion content determination

Zn^{2+}, Mg^{2+} and Ca^{2+} content in buffer and in apo-EAP and apo-BIAP was determined by ICP-AES (inductively coupled plasma atomic emission spectroscopy) (Service Central d'Analyse, CNRS, Vernaison, France). The concentrations of apo-enzymes used for ion content determination were approx. 1 mg/ml corresponding to approx. 15 μm apo-BIAP monomer or 20 μM apo-EAP monomer. Below the limit of detection for Zn^{2+} ($\geqslant 1.5\ \mu M$) and Mg^{2+} ($\geqslant 1.6\ \mu M$), neither of these two ions were detectible in buffer or in both apo-enzymes after two independent analyses. Ca^{2+} was detected in buffer and both apo-enzymes. The average Ca^{2+} concentration in buffer was approx. $15 \pm 10\ \mu M$ after four independent measurements. Enrichment in Ca^{2+} ions was observed in both apo-EAP and apo-BIAP solutions as determined by two independent measurements.

SDS/PAGE and visualization of alkaline phosphatase activity

Electrophoresis was performed on 7.5 % (w/v) SDS/PAGE, by the method of Laemmli [30]. Under mild denaturing conditions, which can preserve the activity of alkaline phosphatase, the samples were prepared in Tris buffer containing 2 % (w/v) SDS, but without the addition of 2-mercaptoethanol or heating before migration. Proteins were stained using Coomassie Brilliant Blue R-250 (Merck, Darmstadt, Germany). After SDS/PAGE, under mild denaturing conditions, the gel was firstly incubated in buffer containing 0.1 M Tris/HCl, pH 9.6, 100 mM NaCl, 5 mM $MgCl_2$, 0.25 mM NBT (nitroblue tetrazolium) and 0.24 mM BCIP (bromochloro-indolyl phosphate) until the bands of sky-blue colour were clearly visible. The BCIP-NBT revealed specifically active alkaline phosphatase; other proteins in the same gel were stained with Coomassie Brilliant Blue R-250 afterwards. The apparent molecular masses of EAP and BIAP were determined under denaturing conditions, they were 45 kDa and 64 kDa for the monomers of EAP and BIAP respectively.

Molecular sieve chromatography assay

The molecular masses of apo-EAP and apo-BIAP were determined by molecular sieve chromatography, using a Superdex™

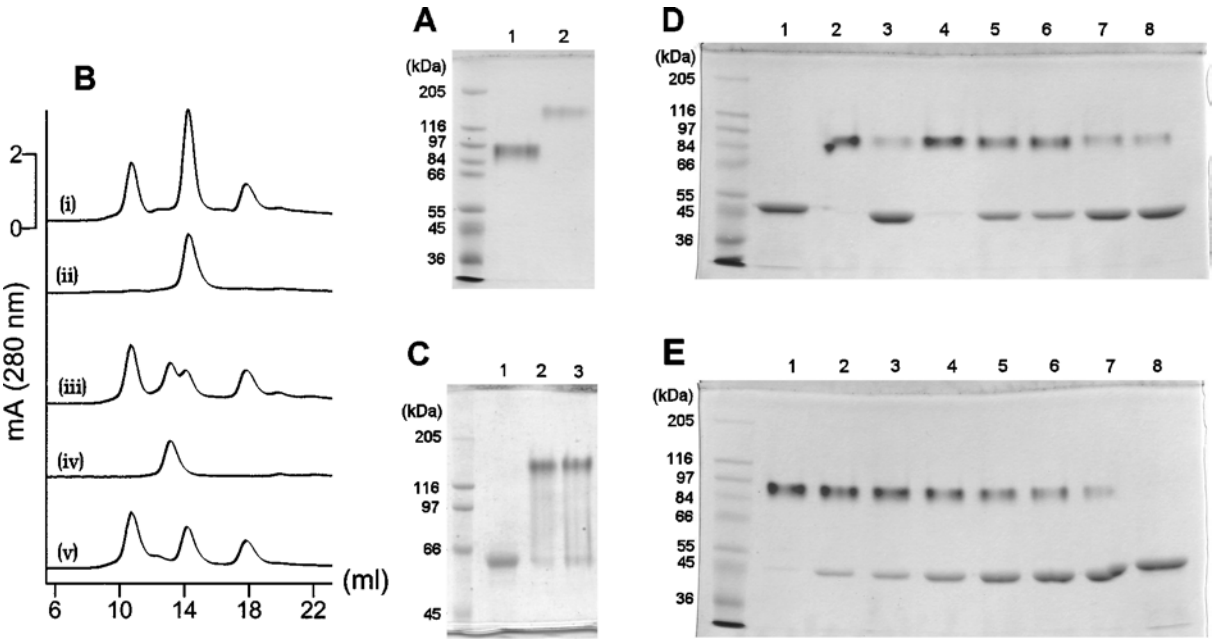

Figure 2 Effect of ions on the dimeric structure of EAP and BIAP analysed by SDS/PAGE and molecular sieve chromatography

(**A**) Determination of the dimeric structure of apo-EAP and apo-BIAP by molecular sieve chromatography. Trace (i), apo-EAP plus protein standards (ferritin 450 kDa, bovine serum albumin 66 kDa and cytochrome *c* 12.5 kDa); trace (ii), native EAP; trace (iii), apo-BIAP plus protein standards; trace (iv), native BIAP; trace (v), protein standards. (**B**) Visualization of active EAP (lane 1) and BIAP (lane 2) by BIAP-NBT staining after SDS/PAGE under mild denaturing conditions. (**C**) Effect of ions on the dimeric structure of BIAP analysed by SDS/PAGE. Lane 1, BIAP in monomeric form under denaturing conditions; lane 2, dimeric BIAP under mild denaturing conditions; lane 3, dimeric apo-BIAP under mild denaturing conditions. (**D**) Effect of ions on the dimeric structure of EAP analysed by SDS/PAGE. EAP or apo-EAP (5 μg) in 10 μl of solution was deposited for each lane, corresponding to approx. 11 μM EAP monomer. Lane 1, EAP prepared under denaturing conditions. Lanes 2–8, samples prepared under mild denaturing conditions in the presence of different ions: lane 2, EAP alone; lane 3, apo-EAP alone; lane 4, apo-EAP + 25 μM Zn^{2+}; lane 5, apo-EAP + 1 mM Mg^{2+}; lane 6, apo-EAP + 5 mM Mg^{2+}; lane 7, apo-EAP + 1 mM Ca^{2+}; lane 8, apo-EAP + 5 mM Ca^{2+}. (**E**) The role of Zn^{2+} in the conversion of monomeric apo-EAP to dimeric EAP. EAP (5 μg) in 10 μl of solution was deposited for each lane, corresponding to approx. 11 μM EAP monomer. Lanes 1–7, samples prepared under mild denaturing conditions in the presence of Zn^{2+} at different concentrations: lanes 1–7, 25 μM, 10 μM, 8 μM, 6 μM, 4 μM, 2 μM and 0 μm; lane 8, apo-EAP prepared under denaturing conditions.

200 HR 10/30 column (Amersham Biosciences), a bed volume of approx. 24 ml and cross-linked agarose and dextran beads 13–15 μm in diameter. The buffer contained 50 mM Tris, 150 mM NaCl and 1 mM EDTA, pH 7.4. The column was incubated overnight with EDTA-containing buffer then equilibrated using 150 ml of the buffer in order to completely eliminate the possibility of ions in the column bed. Protein assays were initiated by injection of 500 μl protein samples, containing 75 μg/ml apo-enzyme with or without three protein standards: 12 μg/ml ferritin (450 kDa), 120 μg/ml BSA (66 kDa) or 50 μg/ml cytochrome *c* (12.5 kDa). Elutions were performed at a flow rate of 0.3 ml/min, at 25 °C. Protein content was monitored by reading the absorbance of the eluted solution at 280 nm. The molecular masses of native EAP and BIAP were determined using Tris buffer without EDTA (50 mM Tris/150 mM NaCl, pH 7.4) as previously described.

IR spectra for apo-enzymes in ^2H_2O buffer

Once apo-enzyme was obtained, it was dried under N_2 and dissolved in ^2H_2O at the same volume as before drying. An aliquot of apo-BIAP stock solution was mixed with the same volume of 20 mM Ca^{2+}, then dried under N_2 and dissolved in ^2H_2O at the same volume as before drying. The sample was incubated overnight at 4 °C. Tris/HCl buffer (20 mM, $p^2H = 7.0$) containing either 20 mM Mg^{2+} and 0.6 mM Zn^{2+} for apo-BIAP, or 20 mM Mg^{2+} and 0.8 mM Zn^{2+} for apo-EAP were prepared. The Zn^{2+} ion concentration was adjusted according to a Zn^{2+}/apo-enzyme monomer ratio of two. The p^2H was measured using a glass electrode and was corrected by a value of 0.4 (p^2H 7.0 = pH 7.4) [31]. A 10 μl apo-enzyme (apo-EAP or apo-BIAP) solution or a 10 μl apo-BIAP solution in the presence of 20 mM Ca^{2+} in ^2H_2O, was added to 10 μl of buffer so that final protein concentration was 10 mg/ml. A 20 μl quantity was then loaded between two circular CaF_2 windows separated by a 50 mm thick Teflon spacer. The IR cell was temperature regulated at 30 °C using a circulating bath. The optical resolution was 4 cm^{-1} but spectral points were encoded every 2 cm^{-1}. Scans (256) were recorded for approx. 4 min. Time delay was 6 min before measuring the first IR spectrum due to the mixing process and transfer of the sample into the IR cell. Series of IR spectra were measured over time. The IR difference spectra correspond to the spectrum of apo-enzyme incubated for the indicated time minus the first spectrum for apo-enzyme recorded after 6 min incubation. Three independent measurements were taken and averaged to obtain spectra with a better signal/noise ratio. The final IR difference spectra were corrected for water-vapour absorption [32,33].

RESULTS

Effect of ions on the stability of EAP and BIAP dimers

It has been reported that apo-EAP remains dimeric at pH 7.4 [34] and we confirmed this finding by molecular sieve chromatography. The elution profile of apo-EAP and that of native EAP were identical, both protein peaks were superimposed on the protein peak of BSA (68 kDa) [Figure 2A, traces (i) and (ii)], showing that both the molecular mass and the global structure of apo-EAP and native EAP were similar. The same experiments were carried out to compare apo-BIAP with native BIAP [Figure 2A, traces (iii) and (iv)], both of their protein peaks were localized at

the 13 ml elution profile, between the protein peak of BSA and that of ferritin (450 kDa), showing that both the molecular mass and global structure of apo-BIAP and native BIAP were similar. These observations indicate that both apo-EAP and apo-BIAP remain dimeric at pH 7.4 despite the lack of ions in their active sites. EAP and BIAP remain active and dimeric after SDS/PAGE under mild denaturing conditions, as revealed by specific BIAP-NBT staining (Figure 2B), showing that these two proteins are resistant to mild SDS/PAGE denaturing conditions, which was confirmed by activity measurements. After 2 h incubation in medium containing 2 % (w/v) SDS, the holoenzymes showed a slight increase in activity of 12 ± 2 % for EAP and 18 ± 4 % for BIAP, confirming that SDS alone is not sufficient to destabilize the active structure of both holoenzymes. The apo-BIAP also kept its dimeric structure after SDS/PAGE under mild denaturing conditions (apparent molecular mass of 150 kDa) (Figure 2C, lane 3), as compared with denatured BIAP (apparent molecular mass of 64 kDa) (Figure 2C, lane 1) and dimeric BIAP (Figure 2C, lane 2).

In apo-EAP, lanes 1 and 2 of Figure 2(D) illustrate the migration of monomeric EAP (apparent molecular mass of 45 kDa; SDS/PAGE under denaturing conditions) and of dimeric EAP (apparent molecular mass of 95 kDa; SDS/PAGE under mild denaturing conditions) as control samples respectively. As shown in lane 3 in Figure 2(D), apo-EAP is mostly in monomeric form, indicating that the apo-EAP dimer is not resistant to the denaturing environment imposed by SDS/PAGE under mild denaturing conditions. The addition of 25 μM Zn^{2+} alone (Figure 2D, lane 4) resulted in almost complete maintenance of the dimeric form of apo-EAP under mild SDS/PAGE conditions. Addition of Mg^{2+} alone resulted in a partial maintenance of the dimeric EAP, and variation in the concentration of Mg^{2+} between 1 mM and 5 mM did not significantly change the rate of maintenance (Figure 2D, lanes 5 and 6). Therefore addition of either Zn^{2+} or Mg^{2+} can reinforce the apo-enzyme dimer. Addition of 1 mM or 5 mM Ca^{2+} alone did not induce any significant dimerization, consistent with the lack of a Ca^{2+} binding site in EAP (Figure 2D, lanes 7 and 8). The ability of Zn^{2+} to affect the rate of maintenance of the dimeric form of apo-EAP was then monitored by SDS/PAGE under mild denaturing conditions (Figure 2E, lanes 1–7). Increasing the Zn^{2+} concentration from 0 to 25 μM showed that a maximal dimerization was almost reached using a Zn^{2+} concentration of 10 μM for 11 μM monomeric apo-EAP. This indicates that two Zn^{2+} ions per dimer of EAP are sufficient to induce the stabilization of the EAP dimer against the denaturing environment imposed by SDS/PAGE under mild denaturing conditions.

Activity recovery of apo-enzymes

The residual activities of apo-EAP and apo-BIAP after the removal of EDTA were approx. 1.5 ± 0.5 % for both apo-enzymes. There was no significant change in activity when apo-enzymes were incubated with 1 μM Zn^{2+}, whereas incubation of apo-enzymes with 5 mM Mg^{2+} allowed them to regain approx. 5 % of their initial activities, suggesting the presence of approx. 5 % residual Zn^{2+} after the removal of EDTA.

To restore alkaline phosphatase activity, 0.45 μM dimeric apo-EAP and 0.016 μM dimeric apo-BIAP, corresponding to an initial activity of 4 units/ml for each enzyme, were first incubated at 37 °C for 1 h in solution containing one of the missing ions: 1 μM Zn^{2+} (Figure 3A) or 5 mM Mg^{2+} (Figure 3B). The other missing ion (Mg^{2+} in Figure 3A and Zn^{2+} in Figure 3B) was then added to the recovery medium. The apo-enzymes were incubated in medium containing both ions for a further hour at 37 °C before measuring the activities. By addition of the Zn^{2+} ion first, then the

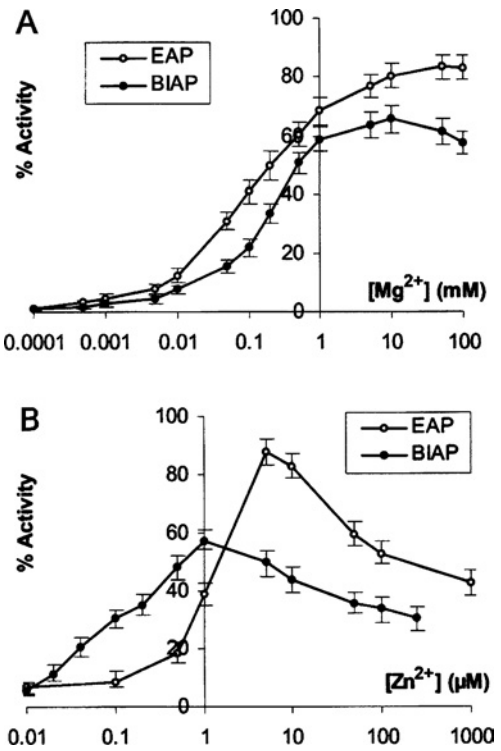

Figure 3 Restoration of activities of apo-enzymes during incubation in medium containing Mg^{2+} and Zn^{2+}

Concentrations of 0.45 μM dimeric apo-EAP (○) and 0.016 μM dimeric apo-BIAP (●) were adjusted so that their initial native activities were 4 units/ml. (**A**) The activities were measured 1 h after addition of 1 μM Zn^{2+}, followed by the addition of 0.1 μM–100 mM Mg^{2+}. (**B**) The activities were measured 1 h after the addition of 5 mM Mg^{2+}, followed by the addition of 10 nM–1 mM Zn^{2+}. The relative activities are expressed as a percentage of the activity of native enzymes and represent the mean $\pm$ S.E.M. of 5 independent assays.

Mg^{2+} ion, we determined the influence of Mg^{2+} on the activity recoveries of these two enzymes (Figure 3A). In the absence of Mg^{2+}, the activity restoration was almost negligible but was enhanced following the increase in Mg^{2+} concentration. Higher Mg^{2+} concentrations, up to 100 mM, induced a slight decrease in activity restoration in the case of BIAP, but not in the case of EAP (Figure 3A). This suggests that EAP is more robust than BIAP towards high Mg^{2+} concentrations. The order of ion additions was reversed to determine the optimal Zn^{2+} concentration for the activity recoveries (Figure 3B). Only a narrow Zn^{2+} concentration range, approx. 1 μM for BIAP or 5 μM Zn^{2+} for EAP, was optimal in regaining maximal activity under these conditions. Pre-incubation of apo-EAP and apo-BIAP with 2 mM Ca^{2+}, before the re-metalating of apo-enzymes in the activity recovery medium, had no effect on the activity restoration of these two apo-enzymes (results not shown), indicating that the active site in both enzymes is specific only for Zn^{2+} and Mg^{2+} ions.

Kinetics of the activity recovery in apo-enzymes

The kinetics of activity restoration of apo-EAP were measured under optimal conditions in medium containing 5 μM Zn^{2+}, 5 mM Mg^{2+} and 0.45 μM apo-EAP corresponding to an initial activity of 4 units/ml, as determined above (Figures 3A and 3B). Apo-EAP recovered approx. 80 % of its initial activity after 3 min incubation. However, total recovery of EAP activity necessitated several days incubation (Figure 4A). In the case of mammalian enzyme, 0.06 μM dimeric apo-BIAP corresponding to

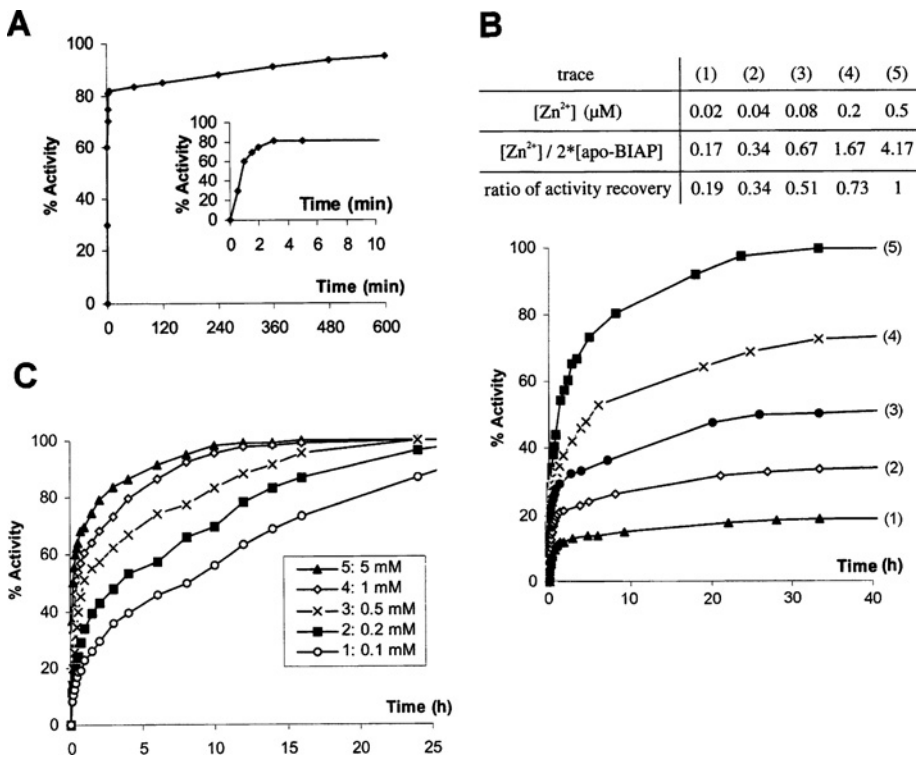

Figure 4 Kinetics of activity recovery of apo-EAP and apo-BIAP

(**A**) Kinetics of activity recovery of apo-EAP. Dimeric apo-EAP (0.45 μM) corresponding to initial activity of 4 units/ml was incubated in medium containing 5 μM Zn^{2+} and 5 mM Mg^{2+} at 37 °C. A small aliquot was taken, according to incubation time, to measure the activity recovery. The activity is expressed as a percentage of the native protein activity. The Figure inset indicates the activity recovery during the first 10 min of incubation. (**B**) The effect of Zn^{2+} on the kinetics of activity recovery of apo-BIAP. Dimeric (0.06 μM) apo-BIAP corresponding to an initial activity of 15 units/ml was incubated at 37 °C in medium containing 5 mM Mg^{2+} and at different Zn^{2+} concentrations ranging from 0.02 to 0.5 μM: trace 1, 0.02 μM (▲); trace 2, 0.04 μM (◇); trace 3, 0.08 μM (●); trace 4, 0.2 μM (×); trace 5, 0.5 μM (■). A small aliquot, was taken according to incubation time, for activity measurement. Inset: table indicating for each trace, the Zn^{2+} concentration, the ratio of Zn^{2+} to dimeric BIAP and the corresponding ratio of final activity recovery after a 40 h incubation. (**C**) The effect of Mg^{2+} on the kinetics of activity recovery of apo-BIAP. Dimeric apo-BIAP (0.06 μM) corresponding to an initial activity of 15 units/ml was incubated at 37 °C in medium containing 0.5 μM Zn^{2+} and at different Mg^{2+} concentrations ranging from 0.1– 5 mM as indicated in (C): trace 1, 0.1 mM (○); trace 2, 0.2 mM (■); trace 3, 0.5 mM (×); trace 4, 1 mM (◇); trace 5, 5 mM (▲). Values shown are the mean of at least four independent assays, with S.E.M. inferior to 10 % of the mean for each panel.

15 units/ml, was incubated in a medium containing 5 mM Mg^{2+} and 0.02 μM–0.5 μM Zn^{2+} (Figure 4B). In this concentration range, the activity restoration increased with Zn^{2+} concentration. As compared with apo-EAP (Figure 4A), apo-BIAP needed a longer incubation time, 6 h, to regain 80 % of its initial activity under optimal conditions (Figure 4B, trace 5). After 25 h, the activity recovery was almost complete (Figure 4B). At the concentration of Zn^{2+} added, which was lower than that of the apo-BIAP monomer, the percentage of the final activity recovery of apo-BIAP was close to the ratio of [Zn^{2+}]/[apo-BIAP monomer] (Figure 4B, traces 1, 2 and 3). This indicates that in the presence of excess Mg^{2+} in the recovery medium, the binding of one Zn^{2+} ion per active site of BIAP is sufficient for this enzyme to regain almost all of its native activity. At a Zn^{2+} concentration of 0.5 μM, the activity restoration of 0.06 μM dimeric apo-BIAP is faster in an increasing Mg^{2+} concentration range of 0.1 mM–5 mM (Figure 4C). The total activity recovery of apo-BIAP was consistently observed within this Mg^{2+} concentration range (Figure 4C). However, at a relatively low Mg^{2+} concentration, as compared with a higher Mg^{2+} concentration, a longer incubation time was required to reach complete activity recovery (Figure 4C, trace 1). The same experiments were performed in the presence of 2 mM Ca^{2+} in the activity recovery medium; the kinetics of activity recovery of apo-EAP and apo-BIAP were not affected by the presence of 2 mM Ca^{2+}, indicating that the Ca^{2+} has no apparent effect on the activity of EAP and BIAP.

Structural changes during the activity restoration of apo-enzymes

To check whether the activity recovery of apo-enzymes was accompanied by secondary structure changes, we measured their IR spectra according to incubation time in the restoration medium. The IR spectrum of apo-BIAP (Figure 5A, top trace) in the amide-I region indicated one peak centered at 1651 cm^{-1} and a shoulder at approx. 1635 cm^{-1}. IR difference spectra for apo-BIAP in the recovery medium were recorded at each hour, up to 5 h (Figure 5A, traces 2–6). An increasing 1458 cm^{-1} broad band associated with an ^{1}H-O-^{2}H band and an N-^{2}H peptide backbone (amide II) was revealed. Only very small changes in the amide-I region were observed and were better shown on an enlarged scale (Figure 5B, traces 2–6). The magnitude of the structural changes to apo-BIAP induced by the fixation of ions was assessed by determining the ratio between the intensity of the amide-I bands of apo-BIAP (Figure 5B, trace 1) and its corresponding amide-I changes induced by addition of ions for different incubation times (Figure 5B, traces 2–6, corresponding to difference spectra measured after 1, 2, 3, 4 and 5 h). The COBSI (change of backbone structure and interaction index) [35], which is the ratio of intensities ($\Delta A/2A$), was 0.0053 for trace 6 (incubation time 5 h). This value corresponded to 2.6 amino acids, per BIAP monomer, involved in the structural changes to BIAP caused by Zn^{2+} and Mg^{2+} binding. The difference spectra for apo-BIAP in the recovery medium, according to incubation

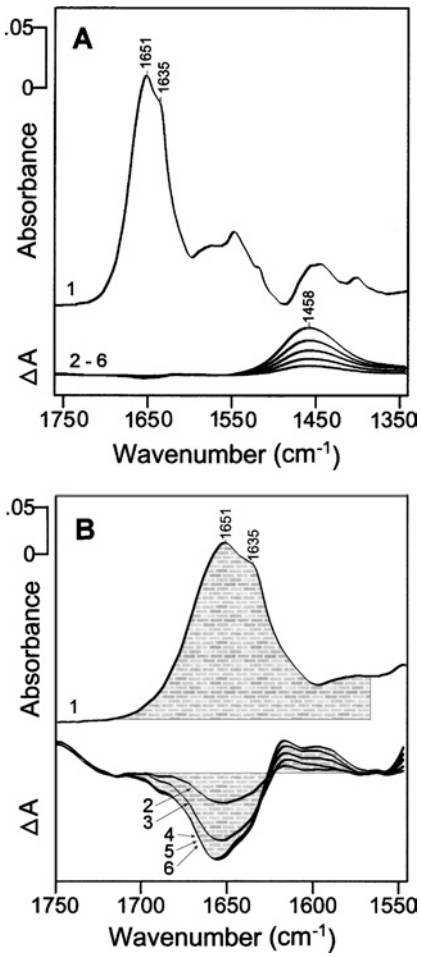

Figure 5 IR difference spectra for apo-BIAP induced by the fixation of Zn^{2+} and Mg^{2+} in ^2H_2O buffer

(**A**) Comparison of structural change to apo-BIAP, induced by the fixation of ions, with the secondary structure of apo-BIAP by IR spectroscopy. Trace 1, IR spectrum for 0.15 mM dimeric apo-BIAP in medium without ions. Traces 2–6, IR difference spectra for 0.15 mM dimeric apo-BIAP with 0.6 mM Zn^{2+} and 20 mM Mg^{2+} at different incubation times (1, 2, 3, 4 and 5 h). Increasing incubation time corresponds to a higher $H/^2H$ exchange rate as indicated by the increase in the 1458 cm^{-1} band. The same absorbance scale was used for all spectra. (**B**) Determination of the magnitude of structural changes to apo-BIAP induced by the fixation of Zn^{2+} and Mg^{2+} ions. Trace 1, IR spectrum for apo-BIAP at time 0. Traces 2–6, IR difference spectra for apo-BIAP at times 1, 2, 3, 4 and 5 h. The absorbance scale was expanded $\times 40$ compared to the scale of the upper spectrum. The calculated intensity of the IR spectrum (trace 1) corresponding to ΔA and the calculated intensity of the IR difference spectrum (trace 6, 5 h) corresponding to ΔA, are indicated by their shaded surfaces. The $\Delta A/2A$ ratio, in the 1760–1600 cm^{-1} region, permitted us to determine the magnitude of peptide backbone structural change to apo-BIAP induced by the fixation of ions [34].

time, indicated that the structural changes slowed down after 2 h incubation (Figure 5B, trace 3). Indeed, after 3 h, there were no further structural changes (Figure 5B, traces 4–6) in contrast with the continuous increase in the 1458 cm^{-1} band (Figure 5A, traces 4–6). Therefore the spectral alterations in the 1750–1550 cm^{-1} region cannot be assigned to ^1H-^2H exchange but were instead associated with small distortions of the peptide backbone or the side chains of the amino acid residues. The IR changes are probably too small to be interpreted in terms of secondary structure alterations, such as the shift of α-helical structure to β-sheet structure. The decrease in the 1651 cm^{-1} band and the concomitant increase in the two other bands located at approx. 1630–1590 cm^{-1} may reflect the formation of stronger hydrogen bonds during recovery of the native structure.

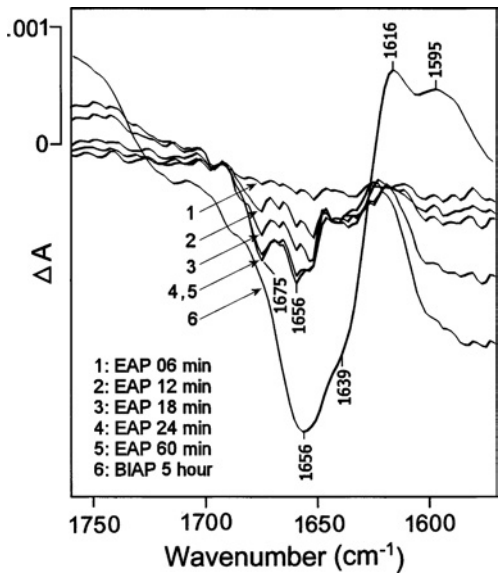

Figure 6 IR difference spectra for apo-EAP induced by the fixation of Zn^{2+} and Mg^{2+} in ^2H_2O buffer

Traces 1–5, IR difference spectra for apo-EAP in recovery medium at different incubation times (6, 12, 18, 24 and 60 min), only the 1750–1550 cm^{-1} region of the spectra is shown. Buffer composition was 20 mM Tris/HCl, 0.4 mM monomeric apo-EAP, $p^2H = 7.0$ containing 0.8 mM Zn^{2+} and 20 mM Mg^{2+}. Trace 6, the IR difference spectrum for apo-BIAP with ions, at 5 h incubation, is identical to trace 6 in Figure 5.

A previous incubation of apo-BIAP with 20 mM Ca^{2+} did not change the shape or magnitude of IR difference spectra for apo-BIAP induced by the addition of Zn^{2+} and Mg^{2+} (results not shown), suggesting that Ca^{2+} did not affect the structure changes to apo-BIAP induced by the addition of Zn^{2+} and Mg^{2+}.

The same experiments were performed using apo-EAP (Figure 6). Since the time delay between addition of the ions and the first measured IR spectra was approx. 6 min, it was not possible to follow the structural changes directly related to the 80 % activity recovery (Figure 4A). Slight structure changes could still be observed in the amide-I region 24 min after measurement of the first IR spectra (Figure 6, trace 1–5). Despite some background interference, two negative bands located at 1675 cm^{-1} and 1656 cm^{-1} could be distinguished on the IR difference spectra for EAP (Figure 6, traces 1–5). These bands could be associated with the protein structure changes, as they stopped after 24 min, whereas the bands corresponding to N-^2H - N-^1H (amide-II) and ^1H-^2H exchange (1458 cm^{-1}) continued to increase with time (results not shown). The structural changes to EAP (Figure 6, traces 1–5) observed in the amide-I region were approx. three times smaller than the structural changes to apo-BIAP (Figure 6, trace 6) under the same conditions. In addition, the shape of their IR difference spectra were distinct.

DISCUSSION

Preparation of apo-enzymes using EDTA

EDTA, an ion chelator, was used to inactivate alkaline phosphatase and was removed from apo-enzymes by several filtration steps through Centricon-30 membranes, to ensure that the final EDTA concentration was sub-nanomolar. Apo-EAP and apo-BIAP are inactive after ion removal, but their activities may be restored by the addition of ions (Figures 3 and 4), indicating that inactivation of EAP and BIAP by EDTA is reversible. An excess amount

of calcium (2–5 mM) did not affect the activity recovery of BIAP and EAP (results not shown), nor the reinforcement of monomer–monomer interaction of apo-EAP under mild SDS/PAGE conditions (Figure 2D), demonstrating that the eventual binding of EDTA to alkaline phosphatase through its ions did not occur. This conclusion was confirmed by the determination of ion content in apo-enzyme by ICP-AES, indicating that Zn^{2+} and Mg^{2+} were not detectable under the technical limits of ICP-AES. These findings show that the recovery of activity of apo-enzymes was mainly associated with Zn^{2+} and Mg^{2+} ions.

Comparison of stability in the dimeric form of apo-EAP and apo-BIAP

Apo-EAP was inactive and dimeric [Figures 2A, traces (i) and (ii)] consistent with the finding that zinc atoms are not essential for maintaining the dimeric form of EAP [34]. Both Zn^{2+} and Mg^{2+} enhance the stabilization of the dimeric form of apo-EAP against mild SDS/PAGE denaturation (Figures 2D and 2E). The affinity of Zn^{2+} for the M1 site of apo-EAP is much higher than for the M2 site [6]. Therefore at very low Zn^{2+} concentration, the cation binds firstly to the M1 site. Given the amount of Zn^{2+} necessary for stabilization of the dimeric form of apo-EAP under mild SDS/PAGE conditions (Figure 2E), which corresponds to a Zn^{2+}/dimeric enzyme ratio of close to 2, it was inferred that binding of Zn^{2+} to apo-EAP occurs in a 'pairwise' manner. In the absence of Mg^{2+}, the binding of one Zn^{2+} ion to the M1 site in one monomer of apo-EAP greatly enhances the affinity of the M1 site in the second monomer for Zn^{2+}, as if two Zn^{2+} ions simultaneously associate to the two M1 sites in apo-EAP. This result is consistent with the positively cooperative process of Zn^{2+} binding to apo-EAP [21,36]. In contrast with apo-EAP, apo-BIAP completely lost its activity but retained its dimeric structure under mild SDS/PAGE conditions (Figure 2C). This finding showed that interactions between the two monomers of eukaryotic BIAP are much stronger than those taking place between the two monomers of prokaryotic EAP, consistent with the 25–30 % similarity between the two enzymes. The presence of additional secondary structure elements in mammalian alkaline phosphatases, including the interfacial-crown-domain, calcium-binding domain and the N-terminal α-helix [17,20,23], and their absence in the prokaryotic enzyme, may account for the difference in the interactions between the two monomers. The effect of cation-binding on the secondary structure of apo-BIAP is relatively weak, only approx. 0.5 % of the overall secondary structure is affected (Figures 5A and 5B), indicating that the core of BIAP is relatively rigid. The rigidity of the active site in BIAP was also observed during the phosphate binding [37].

Comparison of ion sensitivities of prokaryote and eukaryote enzymes

The M1 site is highly specific for Zn^{2+}, whereas a Mg^{2+} ion in the M3 site is essential for catalytic activity of EAP [3,7,9]. A second Zn^{2+} ion in the M2 site enhances the fixation of substrate in the active site, but it is not essential for catalytic activity and does not directly participate in catalysis [38]. The binding of Mg^{2+} in the M3 site can increase the rate of catalysis and thermodynamic stability of EAP [7,9,10] and at high concentrations the Mg^{2+} cation may bind in the M2 site of EAP as well. When Mg^{2+} substitutes Zn^{2+} in the M2 site, a decrease in affinity of EAP for the substrate is observed, however, k_{cat}/K_m is not significantly affected, since a concomitant increase in the k_{cat} value of EAP occurs due to a much easier release of phosphate from its active site [6]. Our observations on ion sensitivities in apo-EAP are consistent with the main conclusions of previous reports. More precisely, at a fixed Mg^{2+} concentration, the enhancement of the activity recovery of apo-EAP with the increase in Zn^{2+} concentration could be interpreted as a progressive binding of Zn^{2+} to the M1 site. At a ratio of two Zn^{2+} ions per apo-EAP dimer, the conformational equilibrium is mostly shifted towards the stabilized dimers (Figure 2E). A higher Zn^{2+} concentration results in saturation of the M1 site, the M2 site then becomes occupied leading to maximum activity restoration. A much higher Zn^{2+} concentration could displace the Mg^{2+} ion from the M3 site, resulting in a decrease in the activity of EAP (Figure 3B). Alternatively, at a fixed Zn^{2+} concentration, the progressive increase in activity recovery of apo-EAP in an increasing Mg^{2+} concentration could correspond to Mg^{2+} binding in the M3 site. A further increase in Mg^{2+} concentration may displace the Zn^{2+} ion from the M2 sites without any significant change in EAP activity (Figure 3A).

The ion sensitivity of apo-BIAP was very similar to that of apo-EAP (Figure 3A and 3B). At the concentration of Zn^{2+} added, which was lower than that of the apo-BIPA monomer, the percentage of the final activity recovery of apo-BIAP was close to the ratio of [Zn^{2+}]/[apo-BIAP monomer] (Figure 4B, traces 1, 2 and 3). This indicates that in the presence of excess Mg^{2+} in the recovery medium, the binding of one Zn^{2+} ion per active site of BIAP is sufficient for this enzyme to regain almost all of its native activity. The M1 binding site of BIAP is highly specific as is the case for EAP. The M3 site must be occupied by Mg^{2+} to obtain optimal activity. The replacement of Mg^{2+} by Zn^{2+} in the M3 site could explain the decrease in the activity recovery of apo-BIAP upon addition of an excess amount of Zn^{2+} (Figure 3B). From these findings, it is tempting to speculate that minor variations in Zn^{2+} concentration (around a few μM) could modulate the activity of alkaline phosphatases under physiological conditions. A higher concentration of Mg^{2+} (up to 50 mM) is needed to observe a slight decrease in activity recovery of apo-BIAP, however, this concentration is outside the expected physiological range between 0.1 and 1.5 mM [39–41], therefore a fluctuation in Mg^{2+} concentration is not expected to affect BIAP activity *in vivo*. The selectivity and sensitivity of the M1 and M3 sites towards cations are very well conserved from *E. coli* to mammalian enzymes despite differences in the rate of activity recoveries and in monomer–monomer interface interaction.

Active structure and native structure of EAP and BIAP

The binding of Zn^{2+} or Mg^{2+} in the active site of apo-EAP is a key factor for the stabilization of its dimeric form (Figures 2D and 2E), and the structural changes to EAP caused by ion binding should not be restricted to the vicinity of the active site, but must extend to the interface region of EAP. As apo-EAP recovers 80 % of its full activity within 3 min (Figure 4A), the binding of Zn^{2+} and Mg^{2+} should be a very fast process. However, due to the roughly 6 min delay in preparing the sample and measuring IR spectra, the results for EAP (Figure 6) could not provide any evidence of such a large shift in domains or conformational change. The small structural changes to EAP, corresponding to less than one amino acid residue, 'stopped' completely after 60 min (Figure 6), but a small continuous increase in activity recovery was still observed (Figure 4A). Proline isomerization is unlikely to be the cause of slow annealing and reactivation during this phase [42]. It has been suggested that the slow conformational changes to EAP, from the high-lability to the low-lability form (native form), on the time scale of days are due to the slow binding of Mg^{2+} to apo-EAP • Zn^{2+} [10]. However, given our findings, the binding of Mg^{2+} to apo-EAP • Zn^{2+} is a fast process, since approx. 80 % of its native activity is recovered in less than 3 min under optimal conditions

(Figure 6). This state in which EAP contains Zn^{2+} and Mg^{2+} ions in their active sites should correspond to the high-lability form of EAP that is not fully active. A longer incubation time is needed to convert the less active and high-lability form of EAP [10] into the native and low-lability form of EAP corresponding to its full stability and activity recovery (Figures 4A and 6) [10]. The shape of the IR difference spectra for apo-BIAP (Figure 6, trace 6) during its slow structural restoration was different from that of apo-EAP (Figure 6, traces 1–5), reflecting different environments surrounding the active site of these two enzymes. However, as in the case of apo-EAP, the secondary structure changes to BIAP did not parallel the kinetics of its activity recovery. The structural changes corresponding to the alteration from two to three peptide backbones slowed down after 2 h incubation of apo-BIAP in the recovery medium and almost stopped after 3 h (Figure 5B), whereas activity recovery of apo-BIAP continuously increased beyond 3 h of incubation (Figures 4B and 4C). This suggests that some of the structural changes associated with the activity recovery for both enzymes are too small to be detected by IR spectroscopy and that distinct and subtle structural changes are required for their optimal activity recoveries.

Calcium and alkaline phosphatase

Calcium can slightly affect the activity of rat osseous plate alkaline phosphatase by binding to Zn^{2+} or Mg^{2+} binding sites only in the absence of these two ions. Then Zn^{2+} or Mg^{2+} may regain their specific binding-sites at a relatively low concentration despite the presence of a relatively high concentration of Ca^{2+} and restore the native activity of the enzyme [43]. The mutation of amino acids that are associated with the inactivation of human tissue non-specific alkaline phosphatase and severe hypophosphatasia could correspond to several amino acids implicated in the coordination of Ca^{2+} in the M4 site [23]. There is no specific binding-site for Ca^{2+} in EAP, whereas such a site exists in mammalian tissue non-specific and placental alkaline phosphatases [17,20,23]. Although the amino acids participating in the coordination of Ca^{2+} are well conserved for the four types of mammalian enzymes, so far the calcium-binding effects on the activity of mammalian intestinal alkaline phosphatase have not been reported. Our findings indicate that the change in Ca^{2+} concentration from 15 ± 10 μM in buffer to a relatively high concentration (up to 20 mM) has no apparent effect on the activity of alkaline phosphatases, or on the kinetics of activity and structure recovery of apo-enzymes induced by Zn^{2+} and Mg^{2+}. Whether the putative calcium-binding site in the case of BIAP is accessible or not remains to be investigated. Alternatively, calcium could bind to BIAP without affecting its activity and overall structure.

In conclusion, although the sensitivity of EAP and BIAP to Zn^{2+} and Mg^{2+} ions was similar, significant differences in dimeric structure stability of apo-enzymes were observed between EAP and BIAP, as well as in the kinetics of their activity and secondary structure recoveries. These differences reflect the distinct environments around the active sites of these two enzymes.

We thank Dr Marie-Hélène le Du for helpful suggestions and discussions. We thank Dr John Carew for correcting the English prior to submission.

REFERENCES

1 Schwartz, J. H. and Lipmann, F. (1961) Phosphate incorporation into alkaline phosphatase of *E. coli*. Proc. Natl. Acad. Sci. U.S.A. **47**, 1996–2005

2 Hull, W. E., Halford, S. E., Gutfreund, H. and Sykes, B. D. (1976) ^{31}P nuclear magnetic resonance study of alkaline phosphatase: the role of inorganic phosphate in limiting the enzyme turnover rate at alkaline pH. Biochemistry **15**, 1547–1561

3 Kim, E. E. and Wyckoff, H. W. (1989) Structure of alkaline phosphatase. Clin. Chim. Acta **186**, 175–188

4 Kim, E. E. and Wyckoff, H. W. (1991) Reaction mechanism of alkaline phosphatase based on crystal structures: two-metal ion catalysis. J. Mol. Biol. **218**, 449–464

5 Coleman, J. E., Nakamura, K. and Chlebowski, J. F. (1983) 65Zn(II), 115mCd(II), 60Co(II), and Mg(II) binding to alkaline phosphatase of *Escherichia coli*. Structural and functional effects. J. Biol. Chem. **258**, 386–395

6 Tibbitts, T. T., Murphy, J. E. and Kantrowitz, E. R. (1996) Kinetic and structural consequences of replacing the aspartate bridge by asparagine in the catalytic metal triad of *Escherichia coli* alkaline phosphatase. J. Mol. Biol. **257**, 700–715

7 Bosron, W. F., Anderson, R. A., Falk, M. C., Kennedy, F. S. and Vallee, B. L. (1977) Effect of magnesium on the properties of zinc alkaline phosphatase. Biochemistry **16**, 610–614

8 Coleman, J. E. (1992) Structure and mechanism of alkaline phosphatase. Annu. Rev. Biophys. Biomol. Struct. **21**, 441–483

9 Janeway, C. M., Xu, X., Murphy, J. E., Chaidaroglou, A. and Kantrowitz, E. R. (1993) Magnesium in the active site of *Escherichia coli* alkaline phosphatase is important for both structural stabilization and catalysis. Biochemistry **32**, 1601–1609

10 Dirnbach, E., Steel, D. G. and Gafni, A. (2001) Mg^{2+} binding to alkaline phosphatase correlates with slow changes in protein lability. Biochemistry **40**, 11219–11226

11 Kam, W., Clauser, E., Kim, Y. S., Kan, Y. W. and Rutter, W. J. (1985) Cloning, sequencing, and chromosomal localization of human term placental alkaline phosphatase cDNA. Proc. Natl. Acad. Sci. U.S.A. **82**, 8715–8719

12 Berger, J., Garattini, E., Hua, J. C. and Udenfriend, S. (1987) Cloning and sequencing of human intestinal alkaline phosphatase cDNA. Natl. Acad. Sci. U.S.A. **84**, 695–698

13 Millan, J. L. and Manes, T. (1988) Seminoma-derived nagao isozyme is encoded by a germ-cell alkaline phosphatase gene. Natl. Acad. Sci. U.S.A. **85**, 3024–3028

14 Weiss, M. J., Henthorn, P. S., Lafferty, M. A., Slaughter, C., Raducha, M. and Harris, H. (1986) Isolation and characterization of a cDNA encoding a human liver/bone/kidney-type alkaline phosphatase. Natl. Acad. Sci. U.S.A. **83**, 7182–7186

15 Manes, T., Hoylaerts, M. F., Muller, R., Lottspeich, F., Holke, W. and Millán, J. L. (1998) Genetic complexity, structure, and characterization of highly active bovine intestinal alkaline phosphatases. J. Biol. Chem. **273**, 23353–23360

16 Redman, C. A., Thomas-Oates, J. E., Ogata, S., Ikehara, Y. and Ferguson, M. A. (1994) Structure of the glycosylphosphatidylinositol membrane anchor of human placental alkaline phosphatase. Biochem. J. **302**, 861–865

17 Le Du, M.-H., Stigbrand, T., Taussig, M. J., Ménez, A. and Stura, E. A. (2001) Crystal structure of alkaline phosphatase from human placenta at 1.8 Å resolution. Implication for a substrate specificity. J. Biol. Chem. **276**, 9158–9165

18 Bradshaw, R. A., Cancedda, F. and Ericsson, L. H. (1981) Amino acid sequence of *Escherichia coli* alkaline phosphatase. Proc. Natl. Acad. Sci. U.S.A. **78**, 3473–3477

19 Kozlenkov, A., Manes, T., Hoylaerts, M. F. and Millán, J. L. (2002) Function assignment to conserved residues in mammalian alkaline phosphatase. J. Biol. Chem. **277**, 22992–22999

20 Le Du, M.-H. and Millán, J. L. (2002) Structural evidence of functional divergence in Human alkaline phosphatase. J. Biol. Chem. **277**, 49808–49814

21 Chlebowski, J. F., Mabrey, S. and Falk, M. C. (1979) Calorimetry of alkaline phosphatase. Stability of the monomer and effect of metal ion and phosphate binding on dimer stability. J. Biol. Chem. **254**, 5745–5753

22 Muller, B. H., Lamoure, C., Le Du, M.-H., Cattolico, L., Lajeunesse, E., Lemaitre, F., Pearson, A., Ducancel, F., Ménez, A. and Boulain, J. C. (2001) Improving *Escherichia coli* alkaline phosphatase efficacy by additional mutations inside and outside the catalytic pocket. Chembiochem. **2**, 517–523

23 Mornet, E., Stura, E. A., Lia-Baldini, A.-S., Stigbrand, T., Ménez, A. and Le Du, M.-H. (2001) Structural evidences for a functional role of human tissue non-specific alkaline phosphatase in bone mineralization. J. Biol. Chem. **276**, 31171–31178

24 Hoylaerts, M. F., Manes, T. and Millán, J. L. (1992) Molecular mechanism of uncompetitive inhibition of human placental and germ-cell alkaline phosphatase. Biochem. J. **286**, 23–30

25 Bossi, M., Hoylaerts, M. F. and Millán, J. L. (1993) Modifications in a flexible surface loop modulate the isoenzyme-specific properties of mammalian alkaline phosphatase. J. Biol. Chem. **268**, 25409–25416

26 Chlebowski, J. F., Armitage, I. M., Tusa, P. P. and Coleman, J. E. (1976) ^{31}P NMR of phosphate and phosphonate complexes of metalloalkaline phosphatases. J. Biol. Chem. **251**, 1207–1216

27 Gettins, P., Metzler, M. and Coleman, J. E. (1985) Alkaline phosphatase. ^{31}P NMR probes of the mechanism. J. Biol. Chem. **260**, 2875–2883

28 Hoylaerts, M. F., Manes, T. and Millán, J. L. (1997) Mammalian alkaline phosphatases are allosteric enzymes. J. Biol. Chem. **272**, 22781–22787

29 Bradford, M. M. (1976) A rapid and sensitive method for the quantitation of microgram quantities of protein utilizing the principle of protein-dye binding. Anal. Biochem. **72**, 248–254

30 Laemmli, U. K. (1970) Cleavage of structural proteins during the assembly of the head of bacteriophage T4. Nature (London) **277**, 680–685
31 Glasoe, P. K. and Long, F. A. (1960) Use of glass electrodes to measure acidities in deuterium oxide. J. Phys. Chem. **64**, 188–190
32 Goormaghtigh, E., Cabiaux, V. and Ruysschaert, J. M. (1994) Subtraction of atmospheric water contribution in Fourier transform infrared spectroscopy of biological membranes and proteins. Spectrochim. Acta Part A **51**, 2137–2144
33 Goormaghtigh, E., Cabiaux, V. and Ruysschaert, J. M. (1994) Determination of soluble and membrane protein structure by Fourier transform infrared spectroscopy. II. Experimental aspects, side chain structure, and H/D exchange. Subcell. Biochem. **23**, 363–403
34 Schlesinger, M. J. and Barrett, K. (1965) The reversible dissociation of the alkaline phosphatase of *Escherichia coli*. I. Formation and reactivation of subunits. J. Biol. Chem. **240**, 4284–4292
35 Barth, A., Von Germar, F., Kreutz, W. and Mäntele, W. (1996) Time resolved infrared spectroscopy of the Ca^{2+}-ATPase. The enzyme at work. J. Biol. Chem. **271**, 30637–30646
36 Chlebowski, J. F. and Mabrey, S. (1977) Differential scanning calorimetry of apo-, apophosphoryl, and metalloalkaline phosphatases. J. Biol. Chem. **252**, 7042–7052
37 Zhang, L., Buchet, R. and Azzar, G. (2004) Phosphate binding in the active site of alkaline phosphatase and the interactions of 2-nitrosoacetophenone with alkaline phosphatase-induced small structural changes. Biophys. J. **86**, 3873–3881
38 Stec, B., Holtz, K. M. and Kantrowitz, E. R. (2000) A revised mechanism for the alkaline phosphatase reaction involving three metal ions. J. Mol. Biol. **299**, 1303–1311
39 Corkey, B. E., Duszynski, J., Rich, T. L., Matschinsky, B. and Williamson, J. R. (1986) Regulation of free and bound magnesium in rat hepatocytes and isolated mitochondria. J. Biol. Chem. **261**, 2567–2574
40 Heinonen, E. and Akerman, K. E. O. (1987) Intracellular free magnesium in synaptosomes measured with entrapped eriochrome blue. Biochim. Biophys. Acta **898**, 331–337
41 Ioannou, P. C. and Konstantianos, D. G. (1989) Fluorometric determination of magnesium in serum with 2-hydroxy-1-naphthaldehyde salicyloylhydrazone. Clin. Chem. **35**, 1492–1496
42 Dirnbach, E., Steel, D. G. and Gafni, A. (1999) Proline isomerization is unlikely to be the cause of slow annealing and reactivation during the folding of alkaline phosphatase. J. Biol. Chem. **274**, 4532–4536
43 Leone, F. A., Ciancaglini, P. and Pizauro, J. M. (1997) Effect of calcium ions on rat osseous plate alkaline phosphatase activity. J. Inorg. Biochem. **68**, 123–127

Received 30 March 2005/5 August 2005; accepted 8 August 2005
Published as BJ Immediate Publication 9 August 2005, doi:10.1042/BJ20050509